The offsets between galaxies and their dark matter in Λ cold dark matter

Matthieu Schaller,[★] Andrew Robertson, Richard Massey, Richard G. Bower
and Vincent R. Eke

Institute for Computational Cosmology, Durham University, South Road, Durham DH1 3LE, UK

ABSTRACT

We use the 'Evolution and Assembly of GaLaxies and their Environments' (EAGLE) suite of hydrodynamical cosmological simulations to measure offsets between the centres of stellar and dark matter components of galaxies. We find that the vast majority (>95 per cent) of the simulated galaxies display an offset smaller than the gravitational softening length of the simulations (Plummer-equivalent $\epsilon = 700$ pc), both for field galaxies and satellites in clusters and groups. We also find no systematic trailing or leading of the dark matter along a galaxy's direction of motion. The offsets are consistent with being randomly drawn from a Maxwellian distribution with $\sigma \leq 196$ pc. Since astrophysical effects produce no feasible analogues for the $1.62^{+0.47}_{-0.49}$ kpc offset recently observed in Abell 3827, the observational result is in tension with the collisionless cold dark matter model assumed in our simulations.

Key words: astroparticle physics – cosmology: theory – dark matter.

1 INTRODUCTION

Observations of one galaxy in cluster Abell 3827 (redshift $z \approx 0.1$; Carrasco et al. 2010) revealed a surprising $1.62^{+0.47}_{-0.49}$ kpc (68 per cent CL) offset between its dark matter and stars (Massey et al. 2015). Such offsets are not observed in isolated field galaxies (Koopmans et al. 2006; Gavazzi et al. 2007).[1] However, offsets inside clusters are consistent with theoretical predictions from models of self-interacting dark matter (SIDM; Spergel & Steinhardt 2000). As galaxies move through a cluster core, interactions with the cluster's dark matter would create a friction and cause a galaxy's dark matter to lag slightly behind its stars (Massey, Kitching & Nagai 2011; Harvey et al. 2014; Kahlhoefer et al. 2014), just like ram pressure causes gas to lag a long way behind stars in the Bullet Cluster (Clowe, Gonzalez & Markevitch 2004; Clowe et al. 2006; Randall et al. 2008; Harvey et al. 2015). Simple simulations tailored to Abell 3827 support this prediction (Kahlhoefer et al. 2015, although current results operate under the limited assumption that the galaxy

is on first infall). Many particle physics models of dark matter naturally predict low level self-interactions (e.g. Tulin, Yu & Zurek 2013; Boddy et al. 2014; Cline et al. 2014; Foot 2014; Hochberg et al. 2014; Khoze & Ro 2014). If the interaction cross-section is considerable $\gtrsim 0.1$ cm^2 g^{-1}, it could also resolve small-scale issues in the predictions of inert, cold dark matter (CDM) models (see review by Weinberg et al. 2015).

Cluster Abell 3827 was originally studied by Williams & Saha (2011) because its light distribution is interesting, with the intention of developing a lens analysis algorithm but not with the expectation of measuring an offset (Williams, personal communication). This is the only galaxy for which an offset has been detected, but it may also be the only galaxy in a cluster for which such a small offset *could* have been detected. The measurement requires three chance circumstances, each individually rare.

(i) The cluster must gravitationally lens a well-aligned background galaxy with a complex morphology. The distribution of foreground dark matter (plus baryons) can be reconstructed from perturbations to this lensed image.

(ii) The cluster must contain a bright galaxy near the Einstein radius. To enable precise measurements, it must intersect the lensed arcs and its mass must be a detectable fraction of the cluster. Since a single cD galaxy generally lies inside any Einstein rings, in practice, this means a cluster with multiple cDs.

(iii) The cluster must be nearby, so small physical separations can be resolved. This reduces its efficiency as a gravitational lens.

The interpretation of the observed offset in such radical terms as SIDM is clouded by the possibility of alternative explanations. First, gravitational lensing is sensitive to the total mass distribution projected along the line of sight. The chance alignment of unrelated

[1] A small number of galaxy quad lenses are not well fitted by standard parametric models of dark matter centred on the optical emission. To fit lens RXS J1131, Claeskens et al. (2006) need to include a 0.044 arcsec offset or $m = 4$ octupole term. With lens COSMOS J09593, Jackson (2008) achieved an acceptable goodness of fit only with a 0.063 arcsec offset and (an unrealistically large) external shear $|\gamma| = 0.25$. However, in these isolated lenses the cause of these poor fits is more likely to be local substructure (Hezaveh et al. 2013). An offset between mass and light would produce a relatively shallow core profile and possibly more detectable central images. Note also that the location of mass peaks is determined much more precisely by strong lensing than by weak lensing (Dietrich et al. 2012; George et al. 2012).

foreground/background structures has created apparently spurious features in other lens systems (Gray et al. 2001; Hoekstra 2003; Host 2012). Similarly, source-lens degeneracies could lead to a similar effect (e.g. Schneider & Sluse 2013, 2014). In Abell 3827, projection effects do not appear to be an issue: of the four galaxies at the centre of the cluster three have a total mass appropriate for their stellar mass, while the fourth (galaxy N1) has a low mass at the location of the stars, but a similarly appropriate total mass slightly offset. Had this been a chance projection, there would be mass at the location of N1 (because of its own, non-offset dark matter) plus a second mass peak (and probably a luminous source). These are not seen.

Secondly, a physical offset might arise even with collisionless dark matter, via the complex astrophysical processes operating in cluster core environments. Gas stripped from and trailing behind an infalling galaxy may self-gravitate and form new stars. This is not consistent with observations of Abell 3827, which has effectively zero star formation rate (Massey et al. 2015, table 1). The different physical extent of dark matter and stars also leads to different dynamical friction, tidal gravitational forces, and relaxation times during mergers. Inside the complex distribution of Abell 3827, even normally linear effects like tidal forces could create or exacerbate small initial offsets. It could also be considered that the galaxy in question is undergoing one of two types of merger.

(i) Coincidentally with the galaxy's arrival near the cluster core, it has recently merged with a former satellite. The tightly-bound stars from the centre of the satellite have not yet had time to mix with the galaxy's stars, and remain as a second peak randomly located within the total system. Simulated analogues of this are not consistent with observations, because the observed galaxy is best fitted in all bands by a *single* Sérsic profile (Massey et al. 2015, table 1).

(ii) The galaxy is about to merge with a more massive halo (the three more central galaxies of similar mass). In simulations, the dark matter from all the systems rapidly mix together into a single smooth halo. This is not consistent with observations, which still show the infalling galaxy's dark matter, *distinct from* and *further away from* the other galaxies' dark matter.[2]

As a control test to determine whether more complex astrophysical effects could build an offset between galaxies and collisionless dark matter, we measure the 3D separation between galaxies' luminous and dark matter in the 'Evolution and Assembly of GaLaxies and their Environments' (EAGLE) suite of hydrodynamical cosmological simulations (Crain et al. 2015; Schaye et al. 2015). These simulations have been calibrated to match the masses and sizes of galaxies in the local Universe. The main EAGLE simulation also reproduces the observed low-redshift luminosity functions (Trayford et al. 2015) and produces an evolution of the galaxy mass function in broad agreement with observations (Furlong et al. 2015). The simulated galaxies display rotation curves in agreement with observations whilst the stellar and dark matter profiles of BCGs match observational data (Schaller et al. 2015a,b). Similarly, the tidal stripping and ram pressure stripping of the satellites as well

as the AGN activity in the BCGs lead to a realistic population of galaxies in clusters (in terms of colours or Star Formation Rate), indicating that the processes that could move matter around are broadly reproduced by the model. The EAGLE simulations are hence, an ideal test-bed to predict the relative positions of galaxies' various components in a statistically meaningful way.

2 METHOD

In this section, we describe briefly the cosmological simulations we analysed and the method used to infer the centre of luminous and dark matter in galaxies.

2.1 The simulation suite

In our study, we use the main EAGLE simulation (Ref-L100N1504) and to explore field galaxies, clusters and groups, and the higher resolution simulation (Recal-L025N0752) to understand the convergence of our results. These cosmological simulations use a state-of-the-art treatment of smoothed particle hydrodynamics and set of subgrid models. The full description of the model is given in Schaye et al. (2015) and the rationale for its parametrization is presented in Crain et al. (2015); we only summarize here the aspects relevant to our study. The simulations assume collisionless dark matter, evolving in a flat ΛCDM cosmology with parameters from *Planck* 2013 (Ade et al. 2014). The low (high) resolution initial conditions are generated at $z = 127$ using second-order Lagrangian perturbation theory in a 100^3 Mpc^3 (25^3 Mpc^3) volume with a dark matter particle mass of 9.7×10^6 M$_\odot$ (1.2×10^6 M$_\odot$) and initial gas particle mass of 1.8×10^6 M$_\odot$ (2.2×10^5 M$_\odot$). The particles are then evolved in time using the GADGET Tree-SPH code (Springel 2005). The Plummer-equivalent gravitational softening is set to $\epsilon = 700$ pc ($\epsilon = 350$ pc at higher resolution).

The subgrid model in the EAGLE simulations includes element-by-element radiative cooling (Wiersma, Schaye & Smith 2009a), star formation obeying the Kennicutt–Schmidt relation (Schaye & Dalla Vecchia 2008), enrichment of the ISM via stellar mass-loss (Wiersma et al. 2009b), feedback from star formation (Dalla Vecchia & Schaye 2012), gas accretion on to supermassive black holes and the resulting AGN feedback (Booth & Schaye 2009; Rosas-Guevara et al. 2013).

2.2 Identification of galaxies and their locations

We find galaxies in the simulation via the SUBFIND algorithm (Springel et al. 2001). We identify all galaxies with stellar mass $M_* > 10^9$ M$_\odot$ at $z = 0$, both in the field and in groups or clusters.

We find the centre of galaxies' matter distributions using an iterative 'shrinking sphere'. We first identify all the star particles for each galaxy. We calculate their centre of mass and the distance of every particle to this centre. We then select only those particles within 90 per cent of the maximal distance to the centre of mass. Repeating this process, the search radius and the number of considered particles decreases in subsequent iterations. This shrinking sphere procedure is repeated until the number of particles reaches 200. This typically corresponds to a sphere of radius $\sim$1 kpc, i.e. slightly larger than the softening length of the simulation. The centre of mass of this final set of particles is considered to be the centre of the galaxy's stellar distribution.[3] Similarly, we define the

---

[2] Allowing a distinct dark matter peak for N1 fits the observations with $\chi^2/\text{dof} = 49.3/23$, Bayesian evidence $\log_{10}(E) = -26.4$, and lens-plane $\langle \text{rms}_i \rangle = 0.26$ arcsec (Massey et al. 2015, table 3). A model without dark matter (but still stellar mass) is strongly disfavoured, with $\chi^2/\text{dof} = 86.1/26$, $\log_{10}(E) = -100.7$ and $\langle \text{rms}_i \rangle = 0.34$ arcsec (R. Massey 2015, personal communication).

[3] As pointed out by Kahlhoefer et al. (2014, 2015), the choice of centroiding algorithm could produce varying results if dark matter does interact. Our
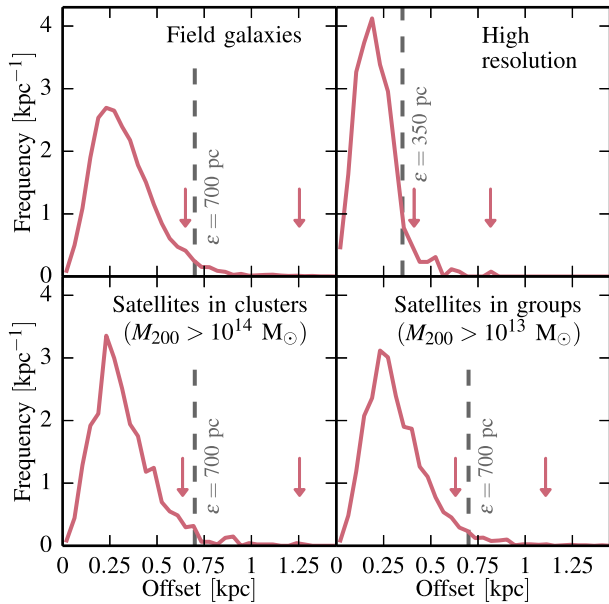
Figure 1. The offset between the centre of the dark matter distribution and stellar distribution for galaxies with a stellar mass $M_* > 10^9$ M$_\odot$. The different panels correspond to field galaxies in the reference simulation (top left), the field galaxies in the higher resolution simulation (top right), satellites in clusters (bottom left) and in groups (bottom right). In each panel the vertical dashed line indicates the softening length used in the simulation. The arrows indicate the position of the 95 per cent and 99.7 per cent percentiles of each distribution. The offset seen is similar in field galaxies and clusters and is of the order of the softening scale of the simulation. Offsets larger than 1.5 kpc correspond to fluctuations greater than 3σ.

velocity of the stellar distribution as the mass weighted velocity of the particles selected in the final iteration of the procedure.

The same procedure is applied to each galaxy's dark matter particles, to calculate the centre of their dark matter distribution. Finally, the offset between the dark and luminous component is defined as the distance between those two centres. We have verified that varying the minimum number of particles to define a galaxy centre from 100 to 500 and the shrinking ratio from 0.5 to 0.99 does not significantly affect our results.

3 OFFSETS BETWEEN DARK MATTER AND STARS

In the EAGLE Ref-L100N1504 simulation there are 12 776 galaxies with mass $M_* > 10^9$ M$_\odot$, 1129 of which are satellites in clusters (haloes with $M_{200} > 10^{14}$ M$_\odot$), 3111 satellites in groups (haloes with $M_{200} > 10^{13}$ M$_\odot$) and 7391 are field galaxies. The higher resolution Recal-L025N0752 simulation contains 618 galaxies above our mass threshold. These four samples will be used to investigate environmental and resolution effects.

3.1 3D offset between dark matter and stellar components

The offsets between the centre of galaxies' dark matter and their stars for our 4 sub-samples of galaxies is shown in Fig. 1. The

identification of mass-weighted peaks in the stellar particles is both robust and the most comparable procedure to the identification of peaks in K-band luminosity-weighted observations (or other infrared bands in the absence of recent star formation).

distributions are consistent with being randomly sampled from a Maxwellian with distribution parameter $\sigma = 196 \pm 2$ pc (main simulation) or $\sigma = 126 \pm 1$ pc (high-resolution simulation). Arrows indicate the position of the 95 and 99.7 (2 and 3σ) percentiles. In both cases, the typical scatter is smaller than the gravitational softening length, indicated by a vertical dashed line.

The distribution of offsets in the Ref-L100N1504 main simulation is remarkably similar for field galaxies (top-left panel) and satellite galaxies in groups or clusters (bottom panels). This indicates that, at our resolution, the offsets are not influenced by environmental effects. Fewer than 5 per cent of all galaxies display an offset larger than the gravitational softening length. Offsets larger than 1 kpc are only found in 59 field galaxies (0.79 per cent) and 17 satellites in groups and clusters (0.54 per cent). Pushing these numbers to offsets larger than 1.5 kpc, we find 15 field galaxies (0.20 per cent) and 2 satellites in groups and clusters (0.06 per cent). A much larger sample of galaxies would, however, be required to characterize robustly the tail of the distribution.

Offsets in the higher resolution Recal-L025N0752 simulation (top-right panel) are smaller, with 95 per cent of the galaxies displaying an offset smaller than 410 pc. Unfortunately, the smaller number of galaxies in that simulation volume does not allow for a thorough discussion of the position of larger percentiles. The results from this simulation indicate that the offsets seen in the main simulation are probably overestimated (at least for field galaxies) and that simulations run at a higher resolution (i.e. with a smaller softening length) would lead to galaxies with smaller offsets between dark matter and stars. However, the decrease in softening length by a factor of 2 between our two simulations has only led to a decrease in median offset by a factor of 1.5, indicating that even higher resolution simulations might not converge towards a negligible offset between components.[4] We nevertheless caution that the softening length is not the only scale setting the resolution of a simulation. Changes in the subgrid parameters and, sometimes, models between different simulations at different resolution are necessary to account for the newly resolved scales and have a non-trivial impact on the analysis of convergence.

3.2 Offset along the direction of motion

If the dark matter-stellar offset in Abell 3827 is due to SIDM, then not only will the centres of the galaxies and dark matter haloes be offset but this offset should also be aligned with the direction of motion of the galaxy with the dark matter trailing the stars. Although the offsets observed in the EAGLE simulation are approaching the resolution limit set by the scale of gravitational softening, it is worth measuring whether the dark matter might be trailing or leading the galaxies in their motion.

The offset between dark matter and stars, projected along the velocity vector of the stars, is shown in Fig. 2. In all four galaxy subsamples, the distribution is symmetric and shows no bias towards leading or trailing motion of the dark matter. The distribution and its mirror image are indistinguishable in a Kolmogorov–Smirnov (KS)

---

[4] The offset of 300–400 pc found by Kuhlen et al. (2013) in high-resolution zoom-in simulation of a single Milky Way-like galaxy is consistent with our findings. That offset from the centre of their dark matter distribution is ∼3 times larger than their softening, indicating that a small but non-zero offset might be found with sufficiently high resolution adopted in the simulations. We note, however, that the dark matter density profile of their galaxy is not monotonic; a result different from what is seen in other simulations.
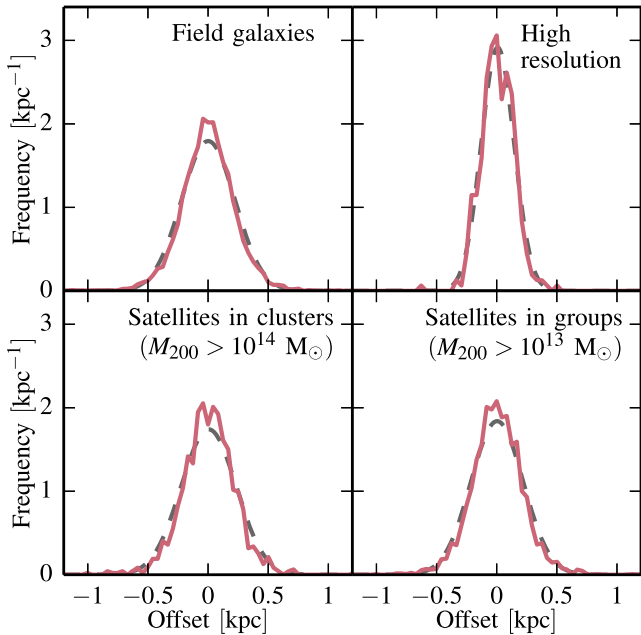
Figure 2. The offset between the centre of the dark matter distribution and stellar distribution along the axis of motion of the stellar distribution for galaxies with a stellar mass $M_* > 10^9\,\mathrm{M_\odot}$. The different panels correspond to the same subsets of galaxies as in Fig. 1. The dashed grey curves in the background show a Gaussian distribution with the same mean and standard deviation as the offset distributions. The distribution of offsets displays no bias towards trailing or leading motion of the dark matter centre with respect to the luminous centre and only deviates from a normal distribution by displaying a positive kurtosis.

test, with a *p*-value larger than 0.9. The scatters are $\sigma \approx 210$ pc (main simulation) or $\sigma \approx 128$ pc (high-resolution simulation), in agreement with those for the Maxwellian 3D offsets. The dashed lines in the figure show Gaussians with the same mean and width as the measured distributions. The distributions of projected offsets seem leptokurtic, with more offsets near 0 than the equivalent Gaussian, but the small number of galaxies in the simulation does not probe the tails of the distribution. The offsets are, thus, consistent with being randomly orientated and unaffected by the motion of the galaxy. Indeed, we find no preferred direction of offset, repeating the experiment by projecting the offset on to other axes like the dark matter velocity, direction to nearest neighbour, direction to cluster centre, etc. All offsets are consistent with random scatter.

3.3 Detailed examination of satellite galaxies in the tail of the distribution

In our sample of satellite galaxies, we found 17 (2) objects out of 3111 presenting an offset larger than 1 kpc (1.5 kpc). It is hence worth exploring whether these are just random fluctuations in the population or whether these larger offsets are seen as the result of an astrophysical process. The offsets of the 17 galaxies display no preferred direction with respect to the direction of motion, with a flat distribution of $\cos(\theta)$, where θ is the angle of the offset from the velocity vector of the galaxy.

The first of the two extreme outliers is a low mass $(M_* = 3.9 \times 10^9\,\mathrm{M_\odot})$ extended galaxy $(r_{50} = 6.9$ kpc). This galaxy is too diffuse at the resolution of the simulation for the centre-finding algorithm to return a sensible answer. Similarly, it would be difficult to find the centre of the light distribution of a galaxy with such a

flat profile in real observations. A galaxy like the one for which an offset has been observed in Abell 3827 is much more massive and less diffuse, making the presence of this specific outlier in our catalogue irrelevant for the scenario we are considering.

The second extreme outlier is a giant elliptical galaxy with stellar mass $M_* = 1.5 \times 10^{11}\,\mathrm{M_\odot}$, located 130 kpc from the centre of its cluster. This galaxy experienced a recent merger with a smaller very concentrated satellite $(M_* \approx 2 \times 10^9\,\mathrm{M_\odot})$.

The dark matter from the two galaxies has mixed, forming a smooth, virialized halo. The stars from the elliptical lie at the centre (within 200 pc) of this dark matter. However, the tightly-bound stars from the centre of the former satellite have not yet had time to mix with the stars from the elliptical. They instead remain as a peak in the outskirts of the stellar light distribution. This merger remnant is thus affecting the measurement of the peak of the light distribution but, at the time of measurement, it does not carry any dark matter. The large perceived offset is a temporary phenomenon due to the difference between the time taken to mix the stars in interacting galaxies and the time needed to mix their dark matter. This is the first merger scenario discussed in the Introduction, and is not consistent with details of the observations (except perhaps a short time window might exist during which distinct dark matter peaks still exist, but are offset from the light. This time window would make Abell 3827 even rarer.)

3.4 Detailed examination of satellite galaxies in the cores of clusters

The simulation contains 50 (11) $M_* > \times 10^{10}\,\mathrm{M_\odot}$ satellite galaxies within the central 100 kpc of groups (clusters). The statistics for this small sample are noisier, but they have a similar offset distribution and distribution of angles between offset and velocity vector as the full sample. The distribution of angles is consistent with uniform and the distribution of offsets has a mean of 310 pc with a 95 percentile at 690 pc, in remarkable agreement with the whole population. This sub-sample and the whole population are virtually indistinguishable in a KS test (*p*-value >0.6).

The closest non-BCG galaxy with $M_* \gtrsim 10^{10}\,\mathrm{M_\odot}$ in the six simulated $M_{200} > 10^{14}\,\mathrm{M_\odot}$ clusters are at clustercentric radii 26 , 92 , 22 , 58 , 82 and 54 kpc. These have offsets between their stars and dark matter of 182 , 223 , 252 , 198 , 320 and 284 pc, in apparently random directions. Looking in more detail at the two objects with the smallest clustercentric position, we find two elliptical galaxies of mass 1.5×10^{10} and $4 \times 10^{10}\,\mathrm{M_\odot}$ with low star formation rate and gas content. They both present an offset between their dark and luminous component smaller than 250 pc, unaligned with their direction of motion nor aligned with the radius to the centre of the cluster. We thus find no feasible analogues for Abell 3827 in the EAGLE simulation.

4 SUMMARY AND CONCLUSION

Motivated by the measurement of a $1.62^{+0.47}_{-0.49}$ kpc offset between the stars and dark matter of a galaxy in Abell 3827 (Massey et al. 2015), we investigated the relative location of these matter components in galaxies from the ΛCDM EAGLE simulation suite. Our results can be summarized as follows.

(i) More than 95 per cent of simulated galaxies have an offset between their stars and dark matter that is smaller than the simulation's gravitational softening length ($\epsilon = 700$ pc). The offsets are smaller still in our higher resolution simulation, indicating that

our measured values are likely upper limits. Even this state-of-the-art cosmological simulation has only just sufficient resolution to compare to the observations.

(ii) Of the extreme objects with resolved offsets, fewer than 0.54 per cent (0.20 per cent) of satellite galaxies in groups and clusters present a separation larger than 1 kpc (1.5 kpc).

(iii) We find no systematic alignment between the direction of the offset and the direction of motion of the galaxies. Dark matter is statistically neither trailing nor leading the stars.

(iv) We find no difference between field galaxies and satellite galaxies in groups and clusters. Astrophysical effects related to a galaxy's local environment play no significant role in producing or enhancing offsets.

(v) We find two types of outliers with extreme offsets: faint galaxies for which the resolution of the simulations does not allow for the robust identification of a centre, and massive galaxies that have recently absorbed a smaller galaxy but have not yet mixed their stellar distributions. Neither of these outlier types match what is observed in Abell 3827.

(vi) Looking specifically at the massive satellite galaxies close to cluster cores, we find no difference between these objects and the overall population of satellites or field galaxies. Environmental effects do not seem to create offsets.

Astrophysical effects, as modelled in the EAGLE simulation, produce no feasible analogue, for the galaxy observed in Abell 3827. Taking the best-fitting value for its observed offset, this galaxy would be a $>3\sigma$ outlier in a ΛCDM universe with collisionless dark matter. Larger, higher resolution simulations will, however, be needed to improve the sampling of the tail of the offset distribution and to assess if the offsets measured in our simulation are biased high by limited numerical resolution.

The observation is so far unique, and finding more systems in which similarly precise measurements can be obtained will be challenging. If more large offsets can be found and larger simulations confirm our findings, the case for an alternative dark matter model (e.g. SIDM) would be compelling. High-resolution simulations including these models of dark matter would also be useful, to understand the processes that might have led to the observed offset in Abell 3827.

REFERENCES

Ade P. A. R. et al., 2014, A&A, 571, A16
Boddy K. K., Feng J. L., Kaplinghat M., Tait T. M. P., 2014, Phys. Rev. D, 89, 115017
Booth C. M., Schaye J., 2009, MNRAS, 398, 53
Carrasco E. R. et al., 2010, ApJ, 715, L160
Claeskens J.-F., Sluse D., Riaud P., Surdej J., 2006, A&A, 451, 865
Cline J. M., Liu Z., Moore G. D., Xue W., 2014, Phys. Rev. D, 90, 015023
Clowe D., Gonzalez A., Markevitch M., 2004, ApJ, 604, 596
Clowe D., Bradač M., Gonzalez A. H., Markevitch M., Randall S. W., Jones C., Zaritsky D., 2006, ApJ, 648, L109
Crain R. A. et al., 2015, MNRAS, 450, 1937
Dalla Vecchia C., Schaye J., 2012, MNRAS, 426, 140
Dietrich J. P., Böhnert A., Lombardi M., Hilbert S., Hartlap J., 2012, MNRAS, 419, 3547
Foot R., 2014, Int. J. Mod. Phys. A, 29, 30013
Furlong M. et al., 2015, MNRAS, 450, 4486
Gavazzi R., Treu T., Rhodes J. D., Koopmans L. V. E., Bolton A. S., Burles S., Massey R. J., Moustakas L. A., 2007, ApJ, 667, 176
George M. R. et al., 2012, ApJ, 757, 2
Gray M. E., Ellis R. S., Lewis J. R., McMahon R. G., Firth A. E., 2001, MNRAS, 325, 111
Harvey D. et al., 2014, MNRAS, 441, 404
Harvey D., Massey R., Kitching T., Taylor A., Tittley E., 2015, Science, 347, 1462
Hezaveh Y., Dalal N., Holder G., Kuhlen M., Marrone D., Murray N., Vieira J., 2013, ApJ, 767, 9
Hochberg Y., Kuflik E., Volansky T., Wacker J. G., 2014, Phys. Rev. Lett., 113, 171301
Hoekstra H., 2003, MNRAS, 339, 1155
Host O., 2012, MNRAS, 420, L18
Jackson N., 2008, MNRAS, 389, 1311
Kahlhoefer F., Schmidt-Hoberg K., Frandsen M. T., Sarkar S., 2014, MNRAS, 437, 2865
Kahlhoefer F., Schmidt-Hoberg K., Kummer J., Sarkar S., 2015, MNRAS, 452, L54
Khoze V. V., Ro G., 2014, J. High Energy Phys., 10, 61
Koopmans L. V. E., Treu T., Bolton A. S., Burles S., Moustakas L. A., 2006, ApJ, 649, 599
Kuhlen M., Guedes J., Pillepich A., Madau P., Mayer L., 2013, ApJ, 765, 10
Massey R., Kitching T., Nagai D., 2011, MNRAS, 413, 1709
Massey R. et al., 2015, MNRAS, 449, 3393
Randall S. W., Markevitch M., Clowe D., Gonzalez A. H., Bradač M., 2008, ApJ, 679, 1173
Rosas-Guevara Y. M. et al., 2013, preprint (arXiv:1312.0598)
Schaller M. et al., 2015a, MNRAS, 451, 1247
Schaller M. et al., 2015b, MNRAS, 452, 343
Schaye J., Dalla Vecchia C., 2008, MNRAS, 383, 1210
Schaye J. et al., 2015, MNRAS, 446, 521
Schneider P., Sluse D., 2013, A&A, 559, A37
Schneider P., Sluse D., 2014, A&A, 564, A103
Spergel D. N., Steinhardt P. J., 2000, Phys. Rev. Lett., 84, 3760
Springel V., 2005, MNRAS, 364, 1105
Springel V., White S. D. M., Tormen G., Kauffmann G., 2001, MNRAS, 328, 726
Trayford J. W. et al., 2015, MNRAS, 452, 2879
Tulin S., Yu H.-B., Zurek K. M., 2013, Phys. Rev. Lett., 110, 111301
Weinberg D. H., Bullock J. S., Governato F., Kuzio de Naray R., Peter A. H. G., 2015, Proc. Natl. Acad. Sci. Cold dark matter: Controversies on small scales, early edn.
Wiersma R. P. C., Schaye J., Theuns T., Dalla Vecchia C., Tornatore L., 2009b, MNRAS, 399, 574
Wiersma R. P. C., Schaye J., Smith B. D., 2009a, MNRAS, 393, 99
Williams L. L. R., Saha P., 2011, MNRAS, 415, 448

This paper has been typeset from a TEX/LATEX file prepared by the author.